ACS Macro Letters

Letter

pubs.acs.org/macroletters

High Refractive Index Inorganic–Organic Interpenetrating Polymer Network (IPN) Hydrogel Nanocomposite toward Artificial Cornea Implants

Quanyuan Zhang,[†] Zheng Fang,[†] Ye Cao,[†] Huamao Du,[†] Hong Wu,[‡] Roger Beuerman,[§] Mary B. Chan-Park,[†] Hongwei Duan,*[,†] and Rong Xu*[,†]

[†]School of Chemical & Biomedical Engineering, Nanyang Technological University, N1.2, 62 Nanyang Drive, Singapore 637459

[‡]Department of Ophthalmology, Second Hospital of Jilin University, Changchun, China 130041

[§]Singapore Eye Research Institute, 11 Third Hospital Ave 168751, Singapore 6223 8458

Supporting Information

ABSTRACT: The use of artificial cornea implants has received increasing attention for treating cornea-related diseases and vision errors due to the low side effects. To achieve long-term successful vision correction, stable and biocompatible materials of high refractive index (RI) need to be developed. Herein, we developed an interpenetrating polymer network (IPN) hydrogel containing well-dispersed ZnS nanoparticles (~3 nm) covalently linked to the first polymer network, poly(2-hydroethyl methacrylate) (PHEMA). The second polymer network used was poly(acrylic acid) (PAA). The resultant ZnS/PHEMA/PAA IPN nanocomposite is clear and transparent at both dry and hydrated states with their RIs measured to be as high as 1.65 and 1.49, respectively. The equilibrium water content of the hydrogel nanocomposite reached 60.2% which is reasonably near to that of cornea. The material exerted minimal cytotoxicity toward primary epidermal keratinocyte cells. The high RI IPN hydrogel nanocomposite developed here might be an excellent candidate for artificial cornea implants.

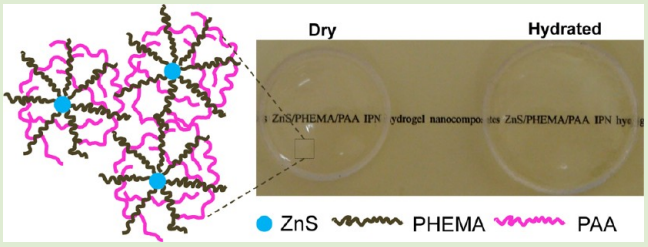

Many people suffer from myopia or hyperopia due to the refractive errors of the cornea all over the world. The use of polymer-based artificial cornea implants holds great promise in treating vision errors as an alternative solution to the irreversible laser-assisted in situ keratomileusis (LASIK) surgery.[1,2] To suit for this application, the polymer material should be biocompatible, colorless, transparent, able to incorporate high water content yet with good mechanical strength, and have a certain refractive index (RI) to allow optical correction.[1] It remains a challenging task to develop polymers that fulfill all of these requirements simultaneously. For decades, the most commonly used material for fabricating artificial cornea was poly(methyl methacrylate) (PMMA), which is a rigid and glassy polymer. With the rapid development in biomedical applications, the use of softer and more hydrophilic polymers toward synthetic corneas has gained increasing attention.[3−9] In contrast to PMMA which does not contain water, large quantities of water incorporated in the cross-linked hydrogel polymers make them resembling the physical characteristics of soft tissues such as high permeability to water-soluble metabolites including glucose, oxygen, and so forth.[7,9] However, the mechanical weakness of high water content hydrogels limits their practical applications. A unique type of interpenetrating polymer network (IPN) hydrogel was reported by Gong et al. via the combination of two different polymer networks.[5,6] These "double networks" hydrogels, with an interpenetrated but independently cross-linked structure, exhibit much enhanced mechanical properties and high resistance to wear despite their high water content. In this regard, the IPN hydrogels of good biocompatibility are considered attractive materials for cornea stroma replacement.

Nevertheless, hydrogel materials with high water contents typically have low RIs since the RI of free water is only 1.33. For example, the porcine collagen based hydrogel with about 90% water was reported with a RI of around 1.35.[10] This is undesirable for vision correction because low RI materials require a relatively thick lens optic to achieve the proper refractive power. An effective way of increasing RIs of polymers is to introduce high RI inorganic nanoparticles into organic matrices. Recently, nanoparticles of TiO_2, ZnO, ZnS, and so forth have been incorporated into the polymer matrix to obtain nanoparticle−polymer composites with high RIs.[11−14] Herein, we for the first time developed IPN hydrogel incorporated with well-dispersed ZnS nanoparticles (NPs) by chemical links. ZnS has a high RI of around 2.36 (at 620 nm) and low absorption coefficient over a broad wavelength range of 400−14000 nm.[15] The covalent bond between ZnS NPs and polymer network

Received: February 17, 2012
Accepted: June 18, 2012
Published: June 26, 2012

   dx.doi.org/10.1021/mz300078y | *ACS Macro Lett.* 2012, 1, 876−881

Scheme 1. Reaction Steps for Fabrication of ZnS/PHEMA/PAA Interpenetrating Polymer Network (IPN) Nanocomposite. (A) Synthesis of the First Network by Polymerization of HEMA Tethered on ZnS Nanoparticles, (B) Formation of the Second Network of PAA Interpenetrating with the First Network, and (C) Schematic Representation of the ZnS/PHEMA/PAA IPN Nanocomposite

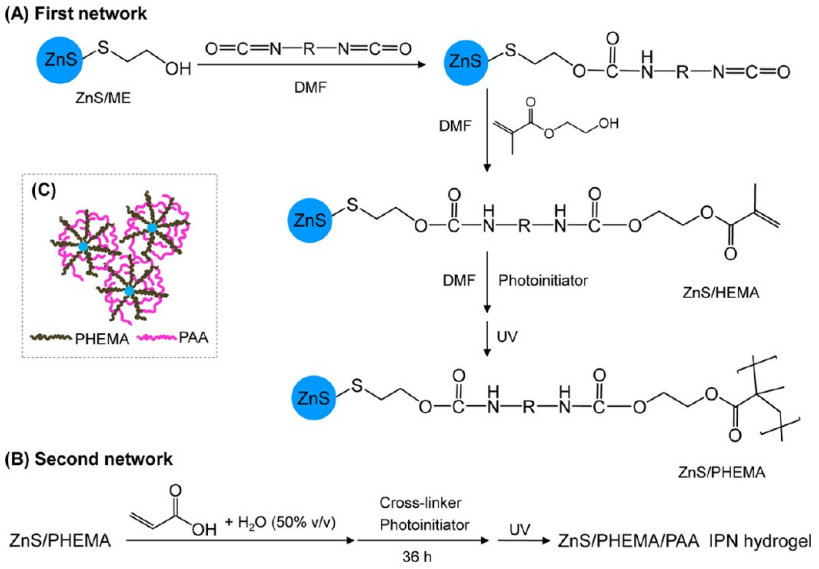

leads to a stable dispersion of NPs, and as a result the composite is optically transparent and clear.

As shown in Scheme 1, the ZnS/poly(2-hydroethyl methacrylate) (PHEMA)/poly(acrylic acid) (PAA) IPN nanocomposite was successfully fabricated by a two-step sequential free radical polymerization. During our synthesis, more than 10 g of mercaptoethanol (ME) capped ZnS (ZnS/ME) NPs was obtained in a single run, and the resultant powder can be readily redispersed in *N*,*N*-dimethylformamide (DMF) to obtain stable and transparent solution which is essential for the subsequent preparation of transparent bulk inorganic/polymer nanocomposites. As shown in high resolution transmission electron microscopy (TEM) images (Figure 1), ZnS/ME NPs of around 3 nm in diameter are well-dispersed. The lattice fringes can be clearly observed, indicating that crystalline ZnS was formed which is favored over their amorphous counterparts due to the associated higher RIs of crystalline materials.[16] The X-ray diffraction (XRD) pattern of ZnS/ME NPs (Figure S1 of the Supporting Information, SI) exhibits three broad diffraction peaks corresponding to the zinc blend structure of ZnS (JCPDS No. 05-0566). The grain size of ZnS NPs estimated by Scherrer's formula is about 3.0 nm based on the (111) peak which is in good agreement with that obtained from TEM. Further functionalization ZnS/ME by 2-hydroxyethyl methacrylate (HEMA) through the linker did not change the crystal structure and crystallinity of ZnS NPs.

FTIR spectra of Zn/ME and Zn/HEMA are shown in Figure 2A; the characteristic stretching vibration of S−H group of ME at 2550−2565 cm^{-1} cannot be observed, indicating that the bond was broken and ME molecules were successfully bound to the ZnS NPs surface.[17,18] The peak at 3460 cm^{-1} of ZnS/ME NPs is due to the vibration of the OH group of ME. After modification of ZnS/ME by 1,4-diisocyanatobutane linker and HEMA, this peak can no longer be observed, since the covalent bond was formed through −OH group of ME. A broad band around 3350 cm^{-1} appeared in the spectrum of ZnS/HEMA which can be attributed to the vibration of NH group of the linker. The characteristic peaks of C═O and C−N vibrations

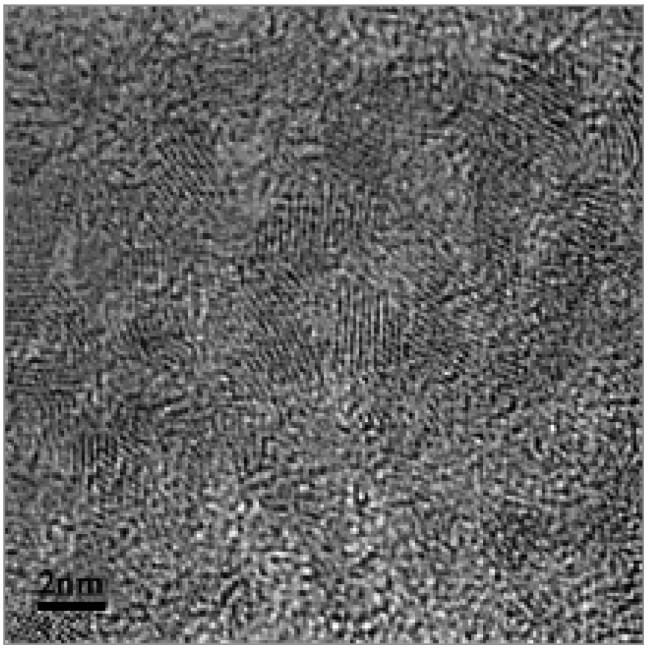

Figure 1. TEM image of mercaptoethanol (ME) capped ZnS nanoparticles.

of amide and C═C stretching vibration of vinyl groups are observed at 1680, 1410, and 1630 cm^{-1}, respectively.[19] Based on these observations, it can be concluded that ME and HEMA molecules were successfully grafted to the surface of ZnS NPs. The characteristic stretching vibration of C═O group of residual DMF molecules can also be observed in the spectrum of ZnS/ME NPs at 1642 cm^{-1}.[17] This peak disappeared after grafting of HEMA. Furthermore, ^{1}H NMR spectra of ZnS/ME and ZnS/HEMA were obtained (Figure S2 of the SI). Both spectra confirmed the presence of ME and HEMA in the samples. Based on thermal analysis results (Figure 2B), the samples started to lose weight at about 200 °C (ZnS/ME) and

dx.doi.org/10.1021/mz300078y | *ACS Macro Lett.* 2012, 1, 876−881

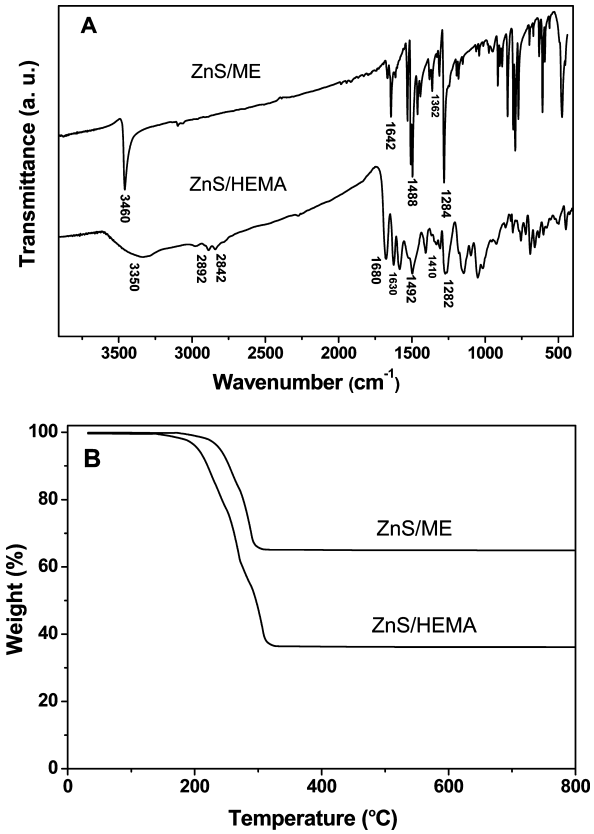

Figure 2. (A) FTIR spectra and (B) TGA results of ME and HEMA capped ZnS NPs.

170 °C (ZnS/HEMA) due to the unstable surface organic compounds. Based on the weight loss percentages, the estimated molar ratio of ME:ZnS and HEMA:ZnS was calculated to be 0.69:1. The chemical analysis results (Table S1 of the SI) by CHNS and ICP methods gave rise to a consistent value of 0.68:1. The cross-sectional area of ME obtained from ChemBio3D Simulation (Gaussian energy minimization) was about 5.35 Å^2. Hence, the estimated percentage of ZnS surface occupied by ME was 94%, indicating that the surface of ZnS was almost saturated by a monolayer of ME.

The covalently grafted organic molecules on the surface of ZnS are expected to improve the compatibility of ZnS NPs with the polymer matrix to avoid phase separation. The first polymer network, PHEMA, was formed by polymerization of HEMA tethered on ZnS NPs (Scheme 1A). The second network, PAA, is more hydrophilic than PHEMA and hence can enhance the water content and at the same time improve the mechanical strength of the hydrogel. The formula of the resultant ZnS/PHEMA/PAA IPN nanocomposite deduced from the chemical analysis data (Table S1 of the SI) was $(ZnS)_{1.00}(PHEMA)_{0.68}(PAA)_{1.51}$. Figure 3 displays the photo images of the as-prepared IPN hydrogel nanocomposite in dry and hydrated states. It can be seen that the both samples are optically clear and transparent. The UV−vis absorption spectrum shown in Figure S3 of the SI indicates that the hydrogel is highly transparent in the range of 315−700 nm. However, the UVB wavelength range (280−315 nm), which is known to cause damage to eyes, is efficiently blocked, suggesting our hydrogel is able to protect UV irradiation to the eyes. The equilibrium water content of the swelled hydrogel was measured to be 60.2%, which is much higher compared to those in the commercial products. For instance, AlphaCor manufactured from a single polymer of PHEMA exhibits relatively low permeability to glucose due to is its low water contents with 45% in the skirt and 35% in the core.[20] To maintain a stable epithelium by the diffusion of nutrients, it is important to have water content near to that of the cornea (78%).[21] The RIs of our nanocomposites were measured to be 1.65 and 1.49 in the dry state and equilibrium hydrated state, respectively. Such RIs are superior to human corneas (1.373−1.380)[22] and the commercial AlphaCor (1.43) as well as those reported by others. For example, Wang et al. developed hydrogel materials from cross-linked polymers of *N*-vinyl-pyrrolidone, 4-vinylpyrimidine, and a vinyl pyridine for manufacturing of intraocular lenses. The RIs of these composites ranged from 1.560 to 1.594 at the dry state, while the values for the hydrated state were not reported.[23] The RIs of recombinant human type I and type III collagen ranged from 1.3451 to 1.3552 with water content between 85.9% and 92.8%.[24] The high RIs of the IPN nanocomposite attained in this study can facilitate the use of a thinner lens optic portion for cornea implants which could lead to much less traumatic surgery for patients and decreased complications and healing time.[25]

The in vitro cytotoxicity studies of the ZnS/PHEMA/PAA IPN hydrogel were carried out using a Transwell cell culture system. The schematic diagram of this system is shown in Figure S4 of the SI, and the morphology of the treated cells by ZnS/PHEMA/PAA IPN hydrogel after calcein AM and EthD-1 staining is displayed in Figure 4. The cells spread quite well with no obvious morphological alteration as compared to the

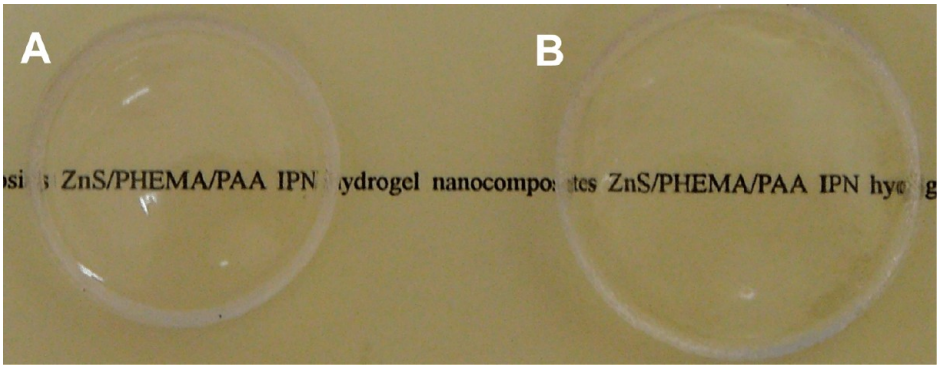

Figure 3. Photo images of (A) dry and (B) hydrated ZnS/PHEMA/PAA IPN nanocomposite.

dx.doi.org/10.1021/mz300078y | *ACS Macro Lett.* 2012, 1, 876−881

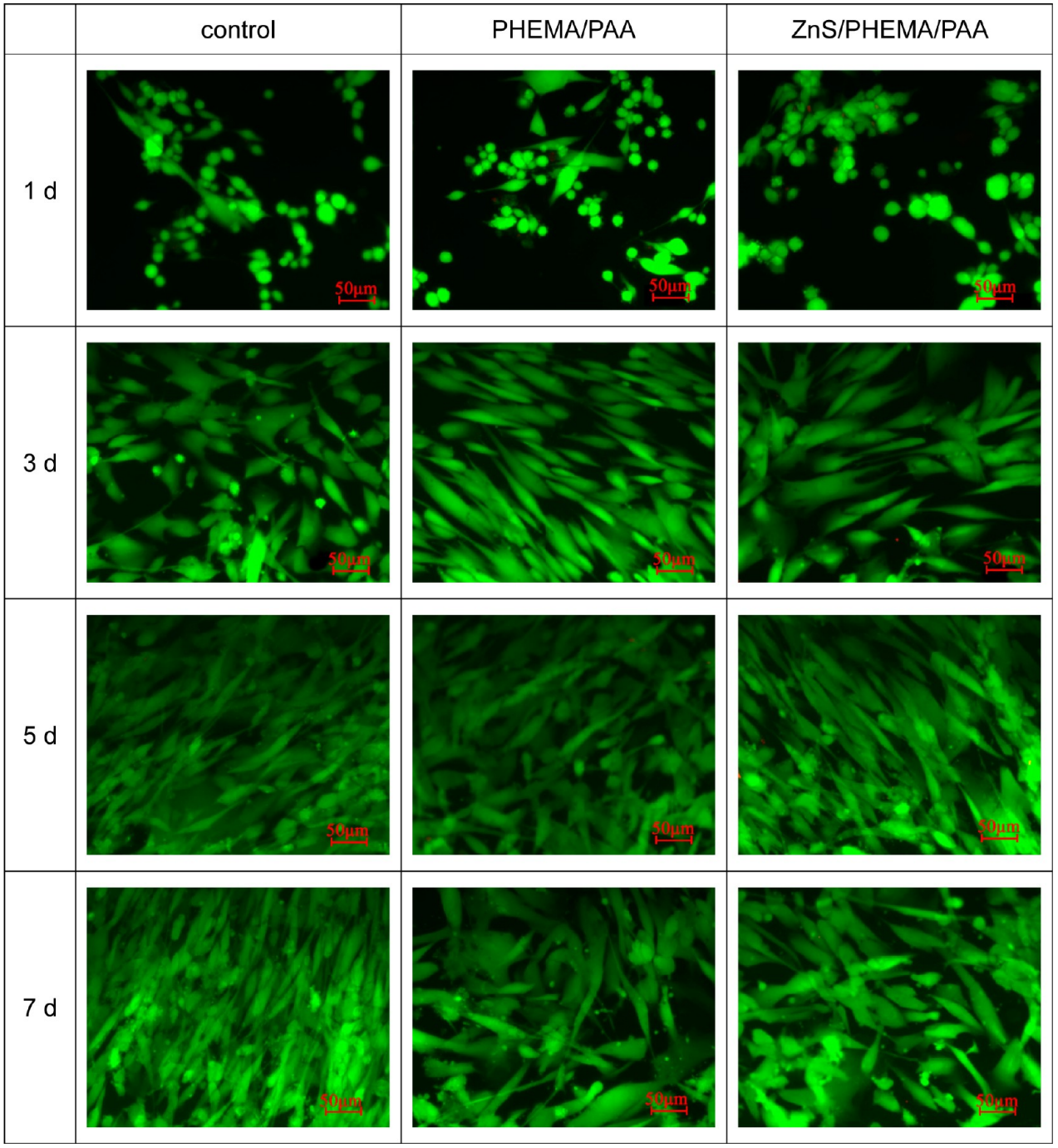

Figure 4. Fluorescence micrographs of calcein AM and EthD-1 stained primary epidermal keratinocytes at different periods of cell culture. Live cells were stained green, while dead cells were red. Cell seeding density: 1.0×10^5 cells/mL.

positive control. The primary epidermal keratinocytes remained the fibroblast shape for both PHEMA/PAA and ZnS/PHEMA/PAA IPN hydrogels. Besides, most of the cells (over 96%) were alive (with green fluorescence) after 7 d, which confirmed high cell viability. Compared with the PHEMA/PAA hydrogel treated cells, the cells on ZnS/PHEMA/PAA IPN hydrogel were similar in calcein AM stained (for live cells), indicating that the introduction of ZnS NPs in PHEMA/PAA IPN hydrogel added little cytotoxicity to primary epidermal keratinocytes. As assessed by the 3-(4,5-dimethylthiazol-2-yl)-2,5-diphenyltetrazolium bromide (MTT) test, cells were allowed to proliferate and increased with culture time. As shown in Figure 5, although less than the positive control, the cell numbers reached confluence within 7 d in the presence of both PHEMA/PAA hydrogel and ZnS/PHEMA/PAA IPN hydrogel, indicating the biocompatibility of both hydrogel materials. The above assay results suggested that the IPN hydrogel exhibited minimal cytotoxicity toward primary epidermal keratinocytes in vitro. The protein adsorption study was carried out using fluorescein isothiocyana (FITC)-labeled bovine serum albumin (BSA) which is highly sensitive approach to confirm the low protein adsorption on the surface. The confocal images (Figure S5 of the SI) show that no obvious change in fluorescence intensity of the hydrogel

dx.doi.org/10.1021/mz300078y | *ACS Macro Lett.* 2012, 1, 876−881

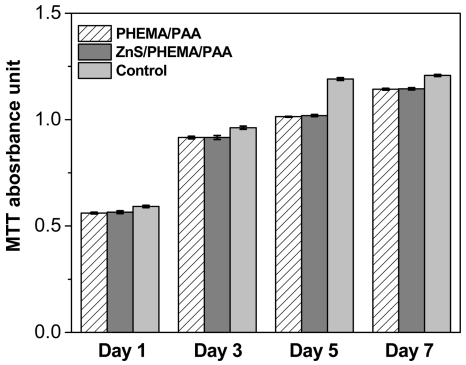

Figure 5. MTT activities (absorbance at 490 nm) of cells cultured for up to 7 d.

compared to that of the control sample, thus supporting the excellent protein-resistant property of the hydrogel. A phase contrast photomicrograph of cells adhered to IPN hydrogel (Figure S6 of the SI) shows that there were no spread cells and only a few scattered cells were found on the surfaces of ZnS/PHEMA/PAA IPN hydrogel. The possibility of Zn^{2+} ion leaching from the hydrogel was investigated by using a Zn-sensitive fluorescent dye, Fluozin3. The PL spectra shown in Figure S7 of the SI indicate that incubating the ZnS/PHEMA/PAA IPN hydrogel with cells for 4 h led to minimal change in fluorescence intensity of the Fluozin3 dye. In contrast, the 100 nM Zn^{2+} solution led to a dramatic increase in fluorescence intensity. Therefore, it can be concluded that the ZnS in the hydrogel is stable under the experimental conditions tested. Finally, the stability of the ZnS/PHEMA/PAA IPN hydrogel was investigated by immersing the hydrogel in deionized water for at least two months. The measured RI and composition remained almost the same. Therefore, the synthetic strategy adopted in this work resulted in a stable composite of nanoparticles and polymers.

In summary, transparent ZnS/PHEMA/PAA IPN hydrogel nanocomposite was successfully synthesized by the introduction of covalently tethered ZnS NPs to the PHEMA/PAA interpenetrating double networks. The equilibrium water content of the hydrogel can reach 60.2%. The RIs of the nanocomposite are as high as 1.65 and 1.49 in the dry and hydrated states, respectively. Cytotoxicity assays, protein adsorption, and cell adhesion tests suggested that the ZnS/PHEMA/PAA IPN hydrogel is biocompatible. The inorganic/polymer nanocomposite developed in this work has great potential as central optic materials in artificial cornea implants.

EXPERIMENTAL METHODS

ZnS/ME synthesis proceeded as follows: ME capped ZnS (ZnS/ME) nanoparticles (NPs) were synthesized in *N*,*N*-dimethylformamide (DMF) according to a modified literature procedure.[26] A 500 mL three-necked round-bottom flask was charged with $Zn(Ac)_2{\cdot}2H_2O$ (22.0 g, 0.1 mol), mercaptoethanol (ME, 11.6 g, 0.148 mol), thiourea (5.5 g, 0.072 mol), and 300 mL of DMF. The solution was refluxed at 160 °C for 10 h under nitrogen with stirring. The resultant mixture was concentrated to 80 mL in a rotary evaporator followed by precipitation using a large amount of ethanol. The white precipitate was collected and thoroughly washed with methanol and then dried in vacuum.

ZnS/HEMA synthesis proceeded as follows: During this step, 3.0 g of ZnS/ME NPs was added to a 25 mL dried round-bottom flask. Then 3.0 mL of DMF was added under nitrogen atmosphere. The mixture was stirred for several min to dissolve the NPs completely. Then, 1.92 g of 1,4-diisocyanatobutane (13.7 mmol) and 0.06 g of dibutyltin dilaurate were dropwise added to the flask. The mixture was kept at room temperature for 4 h under stirring before 1.8 g of 2-hydroxyethyl methacrylate (HEMA, 13.8 mmol) was dropped into the flask. After another 4 h, 10 mL of ethanol was added, and the white precipitate was collected, thoroughly washed with acetone, and then dried in vacuum.

Synthesis of the PHEMA network tethered on ZnS NPs (ZnS/PHEMA) proceeded as follows: ZnS/HEMA NPs were dissolved in DMF at a concentration of 1.0 g/mL. The photoinitiator, 2-hydroxy-2-methyl propiophenone (Darocur 1173, 1% v/v, with respect to the monomer), was added to the solution. The mixture was ultrasonicated for 30 s. This precursor solution was transferred into a Teflon spacer (250 mm in thickness and 20 mm in inner diameter) positioned on a glass plate (1.0 mm thick). After a second glass plate was put on top of the spacer, the solution was exposed to ultraviolet (UV) light (200–2500 nm) for 10 min, during which free radical-induced gelation occurred and the resultant ZnS/PHEMA became insoluble in DMF.

Synthesis of ZnS/PHEMA/PAA interpenetrating polymer network (IPN) nanocomposite proceeded as follows: To incorporate the second network, poly(acrylic acid), PAA, ZnS/PHEMA sample removed from the Teflon spacer was immersed in a 50% (v/v) AA monomer aqueous solution containing the photoinitiator (Darocur 1173, 1% v/v, with respect to the monomer) and the cross-linking agent (TEGDMA, 1% v/v, with respect to the monomer) for 36 h at room temperature. After removing excess AA monomer solution from the surface of ZnS/PHEMA hydrogel, the swollen gel was exposed to the same UV source for 5 min, and a second network, PAA, was polymerized and cross-linked inside the first ZnS/PHEMA hydrogel network. The resultant ZnS/PHEMA/PAA IPN hydrogel was extensively washed and then immersed in deionized water for at least 3 days to remove any unreacted components, as well as to reach equilibrium water content in the swelling state.

ASSOCIATED CONTENT

Supporting Information

Materials, characterization of ZnS NPs, RI measurement and swelling studies, cytotoxicity studies, protein adsorption and cell adhesion study and results, XRD patterns, UV–vis spectrum, ^1H NMR spectra, confocal images after protein adsorption, Zn^{2+} leaching results, and elemental analysis results. This material is available free of charge via the Internet at http://pubs.acs.org.

AUTHOR INFORMATION

Corresponding Author

*E-mail address: hduan@ntu.edu.sg; rxu@ntu.edu.sg.

Notes

The authors declare no competing financial interest.

ACKNOWLEDGMENTS

This work was supported by National Medical Research Council (Grant No. NMRC/NIG/0022/2008) and SingHealth Foundation (Grant No. SHF/09/GMC(1)/012(R)), Singapore.

REFERENCES

(1) Myung, D.; Duhamel, P. E.; Cochran, J. R.; Noolandi, J.; Ta, C. N.; Frank, C. W. *Biotechnol. Prog.* **2008**, *24*, 735–741.
(2) Chirila, T. V. *Biomaterials* **2001**, *22*, 3311–3317.
(3) Crawford, G. J.; Hicks, C. R.; Lou, X.; Vijayasekaran, S.; Tan, D.; Mulholland, B.; Chirila, T. V.; Constable, I. J. *Ophthalmology* **2002**, *109*, 883–889.
(4) Nguyen, K. T.; West, J. L. *Biomaterials* **2002**, *23*, 4307–4314.
(5) Gong, J. P.; Katsuyama, Y.; Kurokawa, T.; Osada, Y. *Adv. Mater.* **2003**, *15*, 1155–1157.

(6) Yasuda, K.; Gong, J. P.; Katsuyama, Y.; Nakayama, A.; Tanabe, Y.; Kondo, E.; Ueno, M.; Osada, Y. *Biomaterials* **2005**, *26*, 4468−4475.
(7) Liu, Y. W.; Gan, L. H.; Carlsson, D. J.; Fagerholm, P.; Lagali, N.; Watsky, M. A.; Munger, R.; Hodge, W. G.; Priest, D.; Griffith, M. *Invest. Ophthalmol. Vis. Sci.* **2006**, *47*, 1869−1875.
(8) Myung, D.; Koh, W.; Bakri, A.; Zhang, F.; Marshall, A.; Ko, J. M.; Noolandi, J.; Carrasco, M.; Cochran, J. R.; Frank, C. W.; Ta, C. N. *Biomed. Microdevices* **2007**, *9*, 911−922.
(9) Duncan, T. J.; Tanaka, Y.; Shi, D.; Kubota, A.; Quantock, A. J.; Nishida, K. *Biomaterials* **2010**, *31*, 8996−9005.
(10) Liu, W. G.; Deng, C.; McLaughlin, C. R.; Fagerholm, P.; Lagali, N. S.; Heyne, B.; Scaiano, J. C.; Watsky, M. A.; Kato, Y.; Munger, R.; Shinozaki, N.; Li, F. F.; Griffith, M. *Biomaterials* **2009**, *30*, 1551−1559.
(11) Lu, C. L.; Cui, Z. C.; Guan, C.; Guan, J. Q.; Yang, B.; Shen, J. C. *Macromol. Mater. Eng.* **2003**, *288*, 717−723.
(12) Lu, C. L.; Cui, Z. C.; Wang, Y.; Li, Z.; Guan, C.; Yang, B.; Shen, J. C. *J. Mater. Chem.* **2003**, *13*, 2189−2195.
(13) Demir, M. M.; Koynov, K.; Akbey, U.; Bubeck, C.; Park, I.; Lieberwirth, I.; Wegner, G. *Macromolecules* **2007**, *40*, 1089−1100.
(14) Lu, C. L.; Cheng, Y. R.; Liu, Y. F.; Liu, F.; Yang, B. *Adv. Mater.* **2006**, *18*, 1188−1190.
(15) Durrani, S. M. A.; Al-Shukri, A. M.; Iob, A.; Khawaja, E. E. *Thin Solid Films* **2000**, *379*, 199−202.
(16) Papadimitrakopoulos, F.; Wisniecki, P.; Bhagwagar, D. E. *Chem. Mater.* **1997**, *9*, 2928−2933.
(17) Hosokawa, H.; Fujiwara, H.; Murakoshi, K.; Wada, Y.; Yanagida, S.; Satoh, M. *J. Phys. Chem.* **1996**, *100*, 6649−6656.
(18) Guo, L.; Chen, S.; Chen, L. *Colloid Polym. Sci.* **2007**, *285*, 1593−1600.
(19) Socrates, G. *Infrared Characteristic Group Frequencies*, 2nd ed.; John Wiley & Sons: New York, 2004.
(20) Gomaa, A.; Comyn, O.; Liu, C. *Clin. Exp. Ophthalmol.* **2010**, *38*, 211−226.
(21) Evans, M. D. M.; Xie, R. Z.; Fabbri, M.; Bojarski, B.; Chaouk, H.; Wilkie, J. S.; McLean, K. M.; Cheng, H. Y.; Vannas, A.; Sweeney, D. F. *Invest. Ophthalmol. Vis. Sci.* **2002**, *43*, 3196−3201.
(22) Patel, S.; Marshall, J.; Fitzke, F. W. *J. Refract. Surg.* **1995**, *11*, 100−105.
(23) Wang, Y. D.; Zhou, S. Q.; Richards, T. P.; Liao, X. G. U.S. Patent 5,480,950, 1996.
(24) Liu, W.; Merrett, K.; Griffith, M.; Fagerholm, P.; Dravida, S.; Heyne, B.; Scaiano, J. C.; Watsky, M. A.; Shinozaki, N.; Lagali, N.; Munger, R.; Li, F. *Biomaterials* **2008**, *29*, 1147−1158.
(25) Crawford, G. J.; Eguchi, H.; Hicks, C. R. *Clin. Exp. Ophthalmol.* **2005**, *33*, 10−15.
(26) Nanda, J.; Sapra, S.; Sarma, D. D.; Chandrasekharan, N.; Hodes, G. *Chem. Mater.* **2000**, *12*, 1018−1024.